Nuclear Instruments and Methods in Physics Research A 830 (2016) 510–514

Contents lists available at ScienceDirect

Nuclear Instruments and Methods in Physics Research A

journal homepage: www.elsevier.com/locate/nima

Laser resonance ionization scheme development for tellurium and germanium at the dual Ti:Sa–Dye ISOLDE RILIS ☆

T. Day Goodacre [a,b,*], D. Fedorov [c], V.N. Fedosseev [a], L. Forster [a], B.A. Marsh [a], R.E. Rossel [a,d,e], S. Rothe [a], M. Veinhard [a]

[a] CERN, CH-1211 Geneva 23, Switzerland
[b] School of Physics and Astronomy, The University of Manchester, Manchester M13 9PL, United Kingdom
[c] Petersburg Nuclear Physics Institute, 188350 Gatchina, Russia
[d] Institut für Physik, Johannes Gutenberg Universität, D-55099 Mainz, Germany
[e] Faculty of Design, Computer Science and Media, Hochschule RheinMain, Wiesbaden, Germany

ARTICLE INFO

Available online 26 October 2015

Keywords:
RILIS
ISOLDE
Germanium
Tellurium
Autoionizing
Laser ionization

ABSTRACT

The resonance ionization laser ion source (RILIS) is the principal ion source of the ISOLDE radioactive beam facility based at CERN. Using the method of in-source laser resonance ionization spectroscopy, a transition to a new autoionizing state of tellurium was discovered and applied as part of a three-step, three-resonance, photo-ionization scheme. In a second study, a three-step, two-resonance, photo-ionization scheme for germanium was developed and the ionization efficiency was measured at ISOLDE. This work increases the range of ISOLDE RILIS ionized beams to 31 elements. Details of the spectroscopy studies are described and the new ionization schemes are summarized.

1. Introduction

1.1. The RILIS at ISOLDE

ISOLDE is an ISOL (isotope separator on-line) type, radioactive ion beam facility based at CERN [1]. A pulsed 1.4 GeV proton beam of up to 2 μA is impacted upon a thick target, creating reaction products via spallation, fragmentation and fission, that are stopped and thermalized within the target material. Depending on the type and composition, the target is heated to between 400 °C and 2400 °C. Higher temperatures reduce the release time of sufficiently volatile elements, which diffuse through the target material and then effuse, via a transfer line, to an ion source.

The resonance ionization laser ion source (RILIS) is the principal ion source of the ISOLDE facility [2]. Laser ion sources of this type are based on two principles: for a particular element, the distribution of the atomic energy levels is unique; and electronic transitions between energy levels can be induced if the atom is illuminated with photons of an energy that matches the transition energy [3]. The RILIS uses multiple laser beams to step-wise excite and then liberate a valence electron from the element of interest. The selectivity of the ionization process follows as a consequence of the element unique distribution of atomic energy levels [4].

The ISOLDE RILIS is a dual Ti:Sa–Dye laser system with six tunable lasers, three Titanium:Sapphire (Ti:Sa) and three dye. All of the lasers produce pulsed light at 10 kHz and are pumped by frequency doubled Nd:YAG (532 nm) lasers, with the option to UV pump the dye lasers at 355 nm. The combination of Ti:Sa and dye lasers with 2ω, 3ω and 4ω frequency conversion enables continuous spectral coverage between 210 nm and 950 nm [2]. An independent 40 W, 10 kHz, TEM_{00}, frequency doubled Nd:YVO_4 (532 nm) Lumera Blaze laser, is available for ionization schemes which rely on a non-resonant ionizing step [5]. A schematic of the RILIS laser system and the experimental setup used for the scheme development is depicted in Fig. 1.

At ISOLDE, the RILIS laser ligth is are transported over a distance of approximately 20 m to converge within a hot-cavity ion source: a tantalum or tungsten tube 3 mm in diameter and 34 mm in length, which is connected to the target container via a transfer line. The entire target and ion source assembly is mounted on an ISOLDE frontend and maintained at a voltage between 20 kV and 60 kV, with a grounded extraction electrode positioned ~60 mm from the exit of the ion source. Resistive heating along the length of the hot cavity creates a voltage drop of ~2 V between the entrance and exit, causing ions to drift towards the penetrating field of the extraction electrode, where they are extracted and accelerated to form an ion beam. Ions generated upstream of the influence of the extraction field are therefore extracted with a low

☆This paper was selected for a special edition of NIMA for LA^{3}NET.

* Corresponding author.
E-mail address: thomas.day.goodacre@cern.ch (T. Day Goodacre).

http://dx.doi.org/10.1016/j.nima.2015.10.066

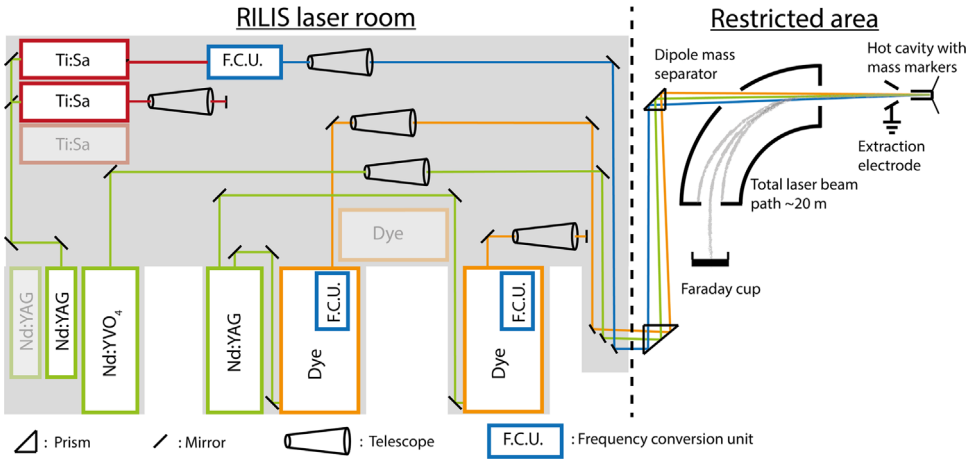

Fig. 1. Schematic of the RILIS layout and the experimental setup for the laser spectroscopy and efficiency measurements.

energy spread (typically <3 V). The ion beam passes through either one or two dipole mass separators, for isotope separation, before being directed to an experiment located in the ISOLDE Hall.

A consequence of the element-selective nature of the RILIS, is that a laser resonance ionization scheme must be developed and tested for each element. It is practical to use stable isotopes for scheme development, rather than relying on radiogenic production with a pulsed proton beam. A mass-marker capillary, containing a stable atomic sample, is connected to the transfer line between the target and ion source hot cavity. During RILIS scheme development, the laser beams are overlapped in the hot cavity and the mass-marker is evaporated while the laser wavelengths are scanned and the ion current is monitored using a Faraday cup located after the mass separator magnet, as depicted in Fig. 1. The laser wavelengths are measured using a HighFinesse WS7 wavemeter.

The spectroscopic studies described here were conducted using laser powers and linewidths identical to standard RILIS operation, to ensure the applicability of the results to on-line radioactive ion beam production at ISOLDE. A comprehensive description of the RILIS laser system can be found in the papers of Fedosseev et al. [2] and Rothe et al. [6].

1.2. Scheme development for the ISOLDE RILIS

The procedure for laser resonance ionization scheme development is described in detail by Fedosseev et al. [7]. The process begins with an assessment of literature data on atomic lines and energy levels. The primary sources of information are the Kurucz and NIST atomic line databases [8,9]. There are a number of relevant factors that determine the suitability of an atomic level or transition for use within an ionization scheme. The possibility to saturate a transition with the available laser power, can be estimated by considering literature data on transition strengths. Candidate transitions are compared to transitions used in existing RILIS ionization schemes, for which the laser power required for saturation has been measured. Thermally populated atomic levels divide the atomic population available to the first excitation step of the laser ionization scheme. In order to determine the optimal starting point of an ionization scheme, the percentage of atoms, P_a, with a valence electron excited to a thermally populated state, a, in the hot cavity environment can be calculated by applying Boltzmann's equation in a form given in the following equations:

$$\phi = g_a \exp(E_a/kT) \tag{1}$$

$$\Phi = \sum_i g_i \exp(E_i/kT) \tag{2}$$

$$P_a = (\phi/\Phi) \times 100 \tag{3}$$

where g is the degeneracy of the atomic state, the subscript a represents a specific atomic state, E is the energy of the atomic state, k is Boltzmann's constant, T is the temperature of the hot cavity in kelvin (K) and the subscript i represents the group of atomic states with a significant thermal population T. Where possible, an excitation path via states with progressively increasing total angular momentum (J) is preferable. This is because the theoretical maximum efficiency of an excitation is greater if the statistical weight $(2J+1)$ of the upper level of the atomic excitation is greater than that of the lower level. The width of an atomic transition in the hot cavity environment must also be considered, this is particularly important if a pronounced hyperfine splitting is expected. An incomplete spectral overlap of the excitation lasers with the resonant transition restricts the accessible atomic population, thereby reducing the ionization efficiency.

2. Tellurium

In addition to ion beam production, the RILIS can also serve as a tool for signal identification. RILIS ionized tellurium is required to enable signal identification for an approved Coulomb excitation experiment investigating ^{116}Te and ^{118}Te [10]. At ISOLDE, tellurium beams have thus far been produced using arc discharge ion sources, which do not offer the element selective capabilities of a RILIS [11]. Recent work at ISOLDE has demonstrated the possibility to couple the RILIS with the VADIS, the ISOLDE variant of the FEBIAD type arc discharge ion source, for laser resonance ionization inside the VADIS anode cavity [12]. The combination, termed the VADLIS or Versatile Arc Discharge and Laser Ion Source, has enabled the possibility of switching to an element selective RILIS-Mode of operation, should either a reduction in isobaric contamination or signal identification be required. The element selectivity of the RILIS provides the option to selectively reduce the tellurium ion rate when operating in RILIS-Mode, by blocking and unblocking one of the laser beams, offering an effective signal identification tool for the analysis of gamma spectra. The experimental setup used for this development work is shown in Fig. 1.

Laser resonance ionization of tellurium was applied previously at ISOLDE as part of a COMPLIS experiment where a two-resonance, three-step scheme of $\{\lambda_1|\lambda_2|\lambda_3\} = \{214.35\text{ nm}|591.53\text{ nm}|1064\text{ nm}\}$ (vacuum wavelengths) was applied [13]. The experiment did not involve ionization inside a hot cavity, thus there were no measured efficiencies applicable to this work. A rich continuum of autoionizing states of tellurium was identified previously using flash pyrolysis and

other non-laser light sources [14–16]. Autoionizing resonances have also been investigated at Oak Ridge National Laboratory (private communication Y. Liu).

Using Eqs. (1)–(3), in a hot cavity ion source at 2300 K we expect a 95% population of the $5p^4\ ^3P_2$ ground state. Thus only schemes involving transitions from the atomic ground state were considered. According to the NIST database [9], the first-step transition from the atomic ground state within the RILIS wavelength range and with the largest photo absorption cross-section, is the 214.281 nm ($5p^4\ ^3P_2 \longrightarrow 5p^3(^4S^o)6s\ ^3S_1^o$) transition. From the $5p^3(^4S^0)6s\ ^3S_1^0$ state, six second-step transitions, also listed in the databases, were observed while scanning a R6G dye laser from 16 805 cm^{-1} to 17 785 cm^{-1}. The four second-step transitions corresponding to the highest ion signals during the scan, were tested as part of three-step, two-resonance ionization schemes, using 532 nm photons from the Blaze laser for non-resonant ionization step. The ion currents recorded for each scheme are compared in Table 1. A search for autoionizing resonances was conducted by replacing the 532 nm third-step laser with a tunable Ti:Sa laser. The search was limited to transitions from the upper level of the two most effective second-step transitions of 573.360 nm and 578.922 nm. A new autoionizing state at 75 181.41 (20) cm^{-1} was identified as part of a {214.281 nm| 573.360 nm| 901.270 nm} scheme.

Comparing the measured ion currents, the autoionizing resonance was a factor of 2.5 more efficient than non-resonant ionization with an estimated 24 W in the ion source. Saturation was verified for the first two resonant transitions, the maximum RILIS laser powers delivered to the ion source for 214 nm light and 573 nm light were estimated to be 25 mW and 6 W respectively. The autoionizing resonance was not saturated with an estimated 1 W of laser light, at 901.270 nm, delivered to the source. The optimal scheme and scans of the 573.360 nm second-step transition and the autoionizing resonance are presented in Fig. 2.

Following this scheme development, the ISOLDE RILIS is now capable of offering signal identification of tellurium related signals, as requested by the IS516 Coulomb excitation experiment, and tellurium ion beam production. Further scheme development, to investigate alternative autoionizing states for a potentially more efficient scheme, is a possibility for future development.

3. Germanium

RILIS ionized germanium beams are required for the study of the β^+/EC decay of ^{64}Ge and ^{66}Ge by total absorption spectroscopy [18]. A three-step, Ti:Sa only, laser ionization scheme with a final step transition to an autoionizing state was developed at ORNL. An efficiency of 3.3% was reported for stable germanium [19].

Based on Eq. (1), and using information from the Kurucz and NIST databases [8,9], the majority of the thermal population at 2300 K is distributed between two atomic states, with 40% lying in the $4s^24p^2\ ^3P_1$ state at 557.134 cm^{-1} and 39% lying in the $4s^24p^2\ ^3P_2$ state at 1409.961 cm^{-1}. Consequently, schemes starting from either $4s^24p^2\ ^3P_1$ or $4s^24p^2\ ^3P_2$ were considered. A 275.459 nm transition ($4s^24p^2\ ^3P_2 \longrightarrow 4s^24p5s\ ^3P_1^0$) was selected from the atomic lines tabulated in literature because of an expectation of saturation and a wavelength that could be produced by frequency doubling the light from a dye laser pumped at 532 nm. From the $4s^24p5s\ ^3P_1^0$ state, four second-step transitions, also documented in literature, were compared as part of two-resonance, three-step schemes with

Table 1
The resonant transitions tested during the tellurium scheme development. Spectroscopic information for known transitions is taken from [9].

Transition (cm^{-1})	Upper state config., term, J	Wavenumber (cm^{-1})	Air wavelength (nm)	Relative ion current
0–46 652.738	$5p^3(^4S^o)6s$, $^3S^0$, 1	46 652.74	214.281	–
46 652.738–63 669.944	$5p^3(^4S^o)7p$, b ^5P, 1	17 017.21	587.478[a]	0.35[b]
46 652.738–63 921.485	$5p^3(^4S^o)7p$, ^3P, 2	17 268.75	578.922	1[b]
46 652.738–63 982.463	$5p^3(^4S^o)7p$, ^3P, 0	17 329.73	576.883[a]	0.24[b]
46 652.738–64 088.997	$5p^3(^4S^o)7p$, ^3P, 1	17 436.26	573.360	0.74[b]
64 088.997–75 181.41 (20)	New	11 092.41 (20)	901.270[a]	2.5

[a] Air wavelengths calculated using the equation of [17].
[b] Ion current measured with ~24 W of 532 nm light delivered to the ion source for the third, non-resonant, ionization step.

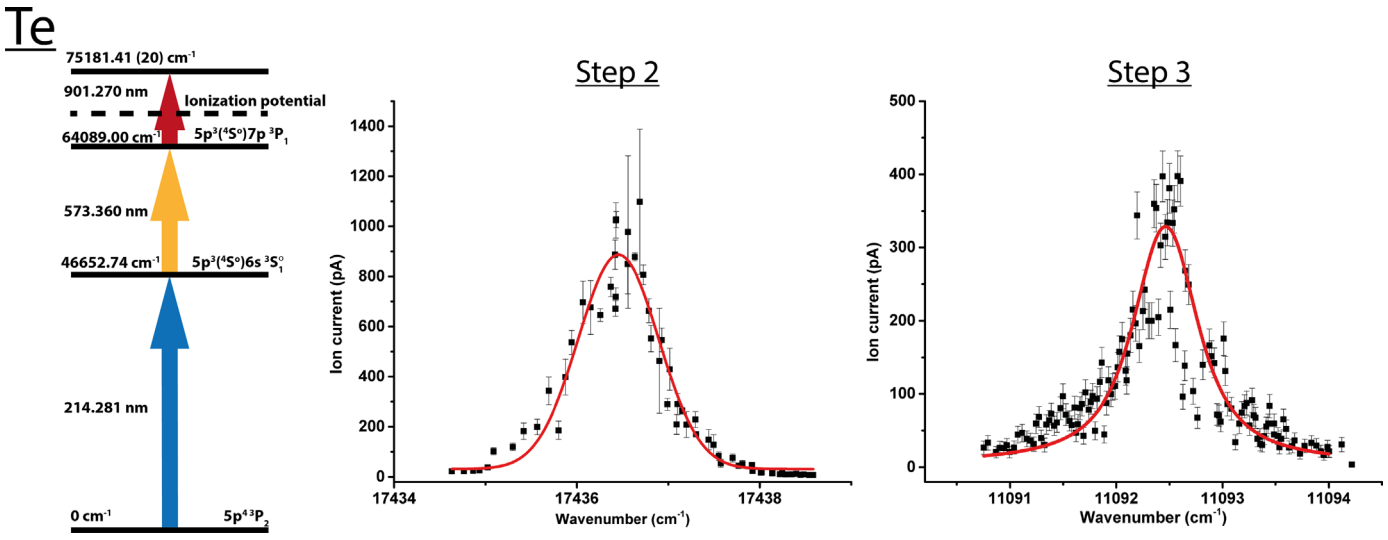

Fig. 2. The optimal tellurium RILIS scheme and laser scans of the second-step and the third-step, autoionizing resonance.

Table 2
The resonant transitions tested during the germanium scheme development. Spectroscopic information is taken from [9].

Transition (cm^{-1})	Upper state config., term, J	Wavenumber (cm^{-1})	Air wavelength (nm)	Relative ion current
1409.961–37 702.305	$4s^24p5s$, $^3P^0$, 1	36 292.34	275.459	–
37 702.305–54 935.848	$4s^24p6p$, ^3D, 1	17 233.54	580.103	0.10[a]
37 702.305–55 235.834	$4s^24p6p$, ^1P, 1	17 533.53	570.178	0.27[a]
37 702.305–55 266.090	$4s^24p6p$, ^3D, 2	17 563.79	569.196	1[a]
37 702.305–55 503.203	$4s^24p6p$, ^3P, 0	17 800.90	561.614	0.26[a]

[a] Ion current measured with ~24 W of 532 nm light delivered to the ion source for the third, non-resonant, ionization step.

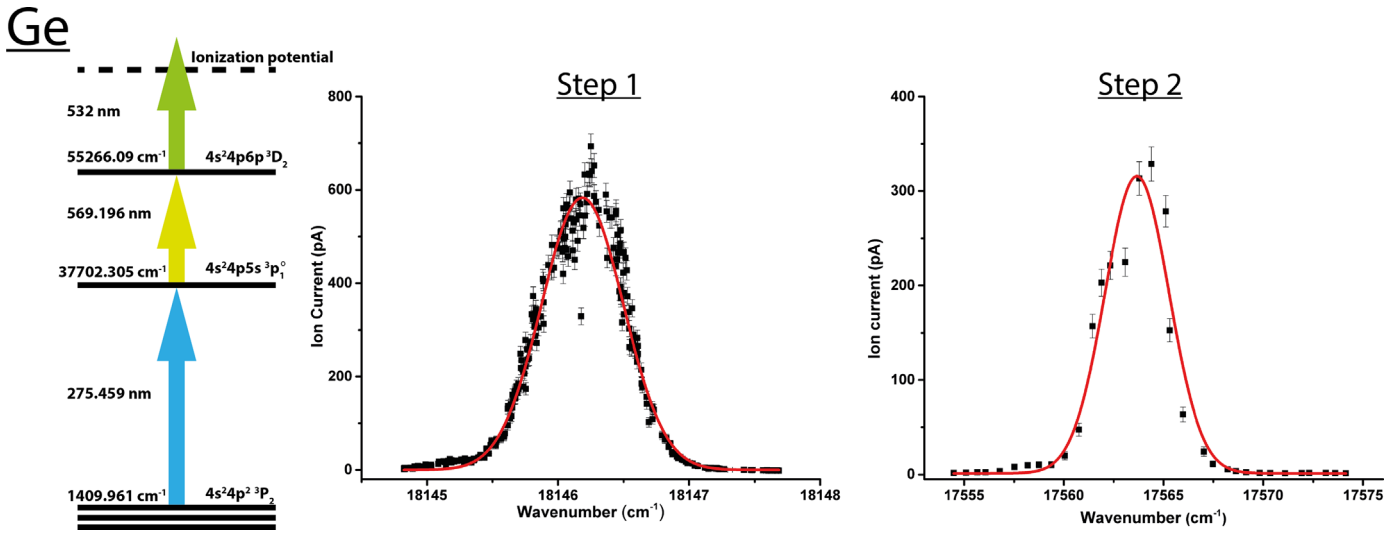

Fig. 3. The most efficient of the tested germanium ionization schemes and scans of the first and second resonances.

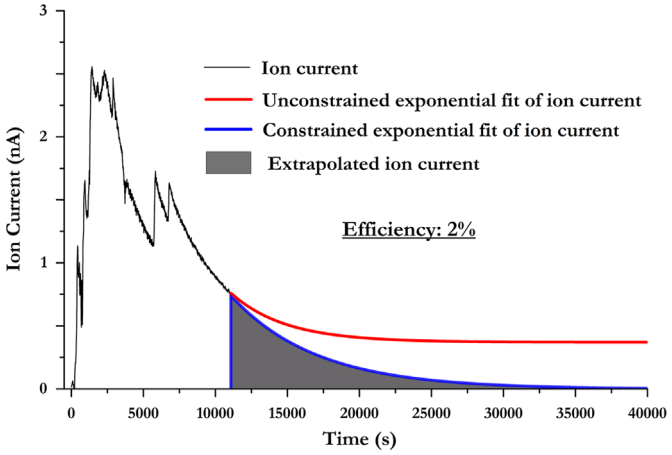

Fig. 4. Laser ionized ^{76}Ge ion current against time during the efficiency measurement.

532 nm photons from the Blaze laser for non-resonant ionization. The results are summarized and compared in Table 2.

The optimal RILIS scheme and laser scans of the first two steps are presented in Fig. 3. Our measurements indicate that the first and second-step transitions were strongly saturated with 580 mW and 14 W respectively on the laser table, estimated to correspond to 300 mW and 5.6 W in the source.

An efficiency measurement was performed for the RILIS scheme depicted in Fig. 3 using a calibrated mass marker of germanium. During the sample evaporation, the laser ion signal was measured on a Faraday cup located after the dipole mass separator magnet. The recorded ion current is plotted against measurement time in Fig. 4. The ion current was integrated over the measurement time in order to extract a lower limit for the ionization efficiency.

The sharp increases in the measured ion current, depicted in Fig. 4, are due to increases in the heating of the calibrated mass marker. Due to time constraints, the measurement was terminated before the sample had been fully evaporated. An extrapolation of the exponential decrease of the ion current was required. A conservative value for the efficiency was determined by constraining the extrapolation to reach zero. An unconstrained extrapolation converged on a 370 pA ion current, suggesting a significant quantity of un-evaporated germanium remaining in the system. The integration over time, of the measured ion current and the constrained extrapolated ion current depicted in Fig. 4, gives a lower limit estimate for the laser ionization scheme efficiency of 2%.

There are two possibilities for improving the efficiency of the germanium ionization scheme: a two-fold efficiency increase could be expected by accessing a larger fraction of the atomic population through the application of an additional first-step laser at 269.134 nm, to excite from the 40% populated (at 2300 K) $4s^24p^2\ ^3P_1$ state to the $4s^24p5s\ ^3P_1^0$ state; or further ionization scheme development to identify useful autoionizing resonances. The application of an additional first-step, to access atoms in a thermally populated state, is standard practice at the ISOLDE RILIS for the ionization of gallium.

4. Conclusion

A new three-step, three-resonance RILIS ionization scheme for tellurium has been developed with a final step transition to a newly identified autoionizing state. The scheme provides sufficient enhancement of the tellurium ion rate to satisfy the needs of signal identification during Coulomb excitation studies at ISOLDE.

With approximately 1 W of laser power delivered to the ion source, the autoionizing resonance was a factor of 2.5 more efficient than a non-resonant ionization step using 24 W of 532 nm light in the source.

Secondly, a new three-step, two-resonance RILIS scheme for germanium was identified and tested using the ISOLDE RILIS. A laser ionization efficiency of $>2\%$ was measured. This efficiency can be increased by the application of an additional first-step to access another thermally populated low-lying atomic energy level, possibly increasing the efficiency of the scheme to $>4\%$. This work extends the range of RILIS ionized beams at ISOLDE to 31 elements.

Acknowledgements

This project has received funding from the European Union's Seventh Framework Programme for research, technological development and demonstration under grant agreements: 262010 (ENSAR), 267194 (COFUND) and 289191 (LA^{3}NET).

References

[1] E. Kugler, Hyperfine Interactions 129 (1/4) (2000) 23.
[2] V.N. Fedosseev, L.-E. Berg, D.V. Fedorov, D. Fink, O.J. Launila, R. Losito, B. A. Marsh, R.E. Rossel, S. Rothe, M.D. Seliverstov, A.M. Sjodin, K.D.A. Wendt, Review of Scientific Instruments 83 (2) (2012) 02A903.
[3] V.S. Letokhov, Laser Photoionization Spectroscopy, 1st ed., Academic Press Inc., London, 1987.
[4] V.N. Fedosseev, Yu. Kudryavtsev, V.I. Mishin, Physica Scripta 85 (May (5)) (2012) 058104.
[5] B. Marsh, T. Day Goodacre, D. Fink, S. Rothe, M. Seliverstov, N. Imai, M. Sjodin, R. Rossel, Suitability Test of a High Beam Quality Nd:YVO4 Industrial Laser for the ISOLDE RILIS Installation, Technical Report, CERN, Geneva, 2013.
[6] S. Rothe, T. Day Goodacre, V.N. Fedosseev, B.A. Marsh, R.E. Rossel, M. Veinhard, K.D.A. Wendt, Laser ion beam production at CERN-ISOLDE: new features—more possibilities. Nuclear Instruments and Methods in Physics Research Section B: Beam Interactions with Materials and Atoms, (Proceedings of The International Conference on Electromagnetic Isotope Separators and Related Topics (EMIS), Grand Rapids, Michigan, USA, May 11–15).
[7] V.N. Fedosseev, B.A. Marsh, D.V. Fedorov, U. Köster, E. Tengborn, Hyperfine Interactions 162 (April (1–4)) (2006) 15.
[8] P.L. Smith, H. Claas, J.R. Esmond, R.L. Kurucz, Atomic spectral line database.
[9] A. Kramida, Yu. Ralchenko, J. Reader, and the NIST ASD Team, NIST atomic spectra database (ver. 5.2), [Online], 2014.
[10] T. Ahn, H. Al-Azri, T. Bloch, P.A. Butler, N. Bree, T. BäcK, S. Bönig, B. Cederwäll, I. D. Darby, J. Diriken, D. O'Donnell, C. Fahlander, L.P. Gaffney, T. Grahn, B. Hadinia, M. Huyse, D. G. Jenkins, A. Johnson, P. Joshi, D. T. Joss, R. Julin, T. Kröll, J. Leske, B.S. Nara Singh, A. Nicholls, R.D. Page, J. Pakarinen, E.S. Paul, N. Pietralla, P. Rahkila, E. Rapisarda, M. Sandzelius, M. Scheck, J. Simpson, J.F. Smith, R. Wadsworth, P. Van Duppen, D. Voulot, F. Wenander, V. Werner, Coulomb Excitation of 116Te and 118Te: a Study of Collectivity Above the Z=50 Shell Gap, Technical Report, CERN-INTC, Geneva, 2011.
[11] U. Köster, U.C. Bergmann, D. Carminati, R. Catherall, J. Cederkäll, J.G. Correia, B. Crepieux, M. Dietrich, K. Elder, V.N. Fedoseyev, L. Fraile, S. Franchoo, H. Fynbo, U. Georg, T. Giles, A. Joinet, O.C. Jonsson, R. Kirchner, Ch. Lau, J. Lettry, H.J. Maier, V.I. Mishin, M. Oinonen, K. Peräjärvi, H.L. Ravn, T. Rinaldi, M. Santana-Leitner, U. Wahl, L. Weissman, Nuclear Instruments and Methods in Physics Research Section B: Beam Interactions with Materials and Atoms 204 (May) (2003) 303.
[12] T. Day Goodacre, J. Billowes, R. Catherall, T.E. Cocolios, B. Crepieux, D. Fedorov, V.N. Fedosseev, J.P. Ramos, L.P. Gaffney, A. Gottberg, K.M. Lynch, B.A. Marsh, T. M. Mendonca, R.E. Rossel, S. Roth, S. Sels, C. Sotty, T. Stora, C. Van Beverene, M. Veinhard, Extending the capabilities of the ISOLDE RILIS by blurring the boundaries between ion sources at ISOLDE, Nuclear Instruments and Methods in Physics Research Section B: Beam Interactions with Materials and Atoms, (Proceedings of The International Conference on Electromagnetic Isotope Separators and Related Topics (EMIS), Grand Rapids, Michigan, USA, May 11–15).
[13] R. Sifi, F. Le Blanc, N. Barré, L. Cabaret, J. Crawford, M. Ducourtieux, S. Essabaa, J. Genevey, G. Huber, M. Kowalska, C. Lau, J.K.P. Lee, G. Le Scornet, J. Oms, J. Pinard, B. Roussière, J. Sauvage, M. Seliverstov, H. Stroke, Hyperfine Interactions 171 (July (1–3)) (2006) 173.
[14] J. Berkowitz, C.H. Batson, G.L. Goodman, Physical Review A 24 (July (1)) (1981) 149.
[15] A.M. Cantú, M. Mazzoni, Y.N. Joshi, Physica Scripta 27 (April (4)) (1983) 261.
[16] M. Mazzoni, A.M. Cantu, Y.N. Joshi, Journal of Physics B: Atomic and Molecular Physics 16 (September (17)) (1983) 3183.
[17] K.P. Birch, M.J. Downs., Metrologia 30 (January (3)) (1993) 155.
[18] E. Nacher, C. Domingo, J.A. Algora, A. Briz, M. Carmona, A. Illana, A. Jungclaus, A. Peria, V. Pesudo, G. Ribeiro, J. Sanchez-del Rio, P. Sarriguren, J. Taprogge, O. Tengblad, J. Agramunt, G. Guibrone, V. Guadilla, A. Montaner, S.E.A. Orrigo, B. Rubio, J.L. Tain, E. Valencia, J. Jose, A. Parikh, L.M. Fraile, I. Marroquin, O. Moreno, B. Olaizola, V. Paziy, J.M. Udias, V. Vedia, M.J.G. Borge, T. Day Goodacre, V. Fedosseev, B. Marsh, E. Rapisarda, T. Stora, W. Gelletly, P. Regan, Z. Podolyak, S. Rice, R Orlandi, M. Carmona, et al., Beta Decay of the N=Z, rp-Process Waiting Points: 64Ge, 68Se and the N=Z+2: 66Ge, 70Se for Accurate Stellar Weak-Decay Rates, Technical Report, CERN-INTC, Geneva, 2013.
[19] Y. Liu, C. Baktash, J.R. Beene, H.Z. Bilheux, C.C. Havener, H.F. Krause, D. R. Schultz, D.W. Stracener, C.R. Vane, K. Brück, Ch. Geppert, T. Kessler, K. Wendt, Nuclear Instruments and Methods in Physics Research Section B: Beam Interactions with Materials and Atoms 243 (February (2)) (2006) 442.